Supplementary Material:
Calibration of the Atomic Oxygen Exposure facility

For the calibration of the test stand and the subsequent test campaign, a set of the following parameters was fixed to the values given in table S1: The pressure inside the plasma chamber p_P, which is controlled by the inlet flow of molecular oxygen via a needle valve. The pressure inside the vacuum chamber p_{vc}, which is directly influenced by p_P. The Power P_{mv} of the microwave generator, dissipated into the plasma and the temperature T_s of the samples.

Table S1: Fixed set of parameters for the calibration and the test campaign

parameter	value	uncertainty	unit
p_P	1	± 0.1	[mbar]
p_{vc}	1.1×10^{-5}	$\pm 0.33 \times 10^{-5}$	[mbar]
P_{mv}	200	±2	[W]
T_s	303	10	[K]

The pressure inside the plasma chamber p_P was precisely controlled via a manual needle valve and was measured with a Pfeiffer TPR 270 Pirani Gauge with an uncertainty of ± 0.1 mbar. However, as the plasma pressure highly depends on the temperature of the laboratory environment and differs between day and night, it was not the pressure itself that was reproducibly controlled but the position of the needle valve. The difference in pressure between night and day was in the range of the measurement uncertainty.

The pressure inside the vacuum chamber p_{vc} was measured with a Pfeiffer PKR 251 with an uncertainty of $\pm 0.33 \times 10^{-5}$ mbar. In contrast to p_P a change in pressure could not be observed between night and day or was smaller than the resolution of the measurement device.

The microwave power P_{mv}, dissipated into the plasma was measured with the integrated measurement unit of the microwave generator with an uncertainty of ± 2 W. The signal itself remained stable over the entire calibration and test campaign.

The parameters in table S1 were used for every test during calibration and the test campaign. It has to be noted that the temperature of the sample as well as the environmental pressure in the vacuum chamber are not comparable for a mission in LEO.

Fluence of Atomic Oxygen

The fluence of atomic oxygen of the ATOX test stand was determined, using samples of Kapton® HN 200 from Dupont. Kapton® is a polyimide and known to be susceptible to atomic oxygen. Its erosion rate E_K is well documented in the literature and determined experimentally in LEO. It is specified with 3×10^{-24} cm³/Atom [25], without a measurement uncertainty provided.

Measuring the difference in mass of the samples Δm_K before and after atomic oxygen exposure, the atomic oxygen fluence F of the test stand can be computed using eq. (S1)

$$F = \frac{\Delta m_K}{A_K \rho_K E_K}$$

(S1)

with the exposed area A_K and the density of Kapton® ϱ_K = 1.43 g/cm³. Limiting the exposed area of the sample, a square shaped aperture made of aluminium with a side length of 10 ± 0.5 mm was put on top of the sample holder (see Fig. S1).
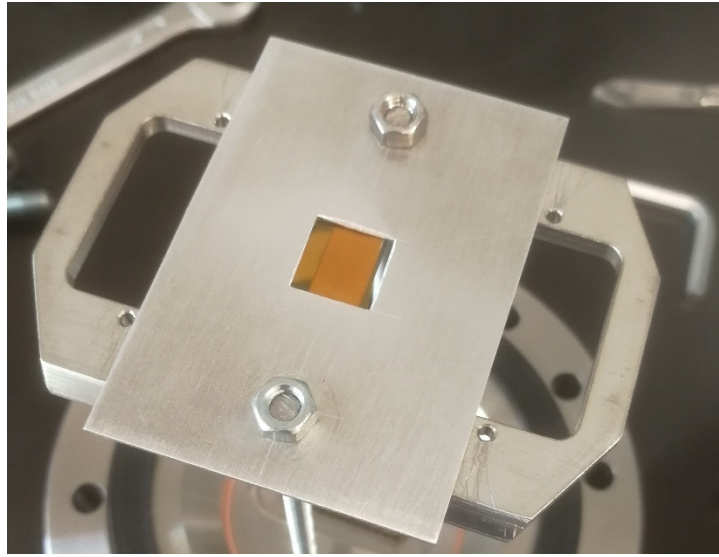

Figure S1: Sample holder with aluminium aperture for setting a limited exposed area; Kapton® HN 200 sample inside

The mass of the samples before and after the test was measured with a Microcrystal 300 precision scale from Gilbertini with a resolution of 1 µg. However, an investigation of the reliability of the measurement was required. Following the laws of propagation of uncertainty, the indirect measurement of fluence is highly sensitive and directly proportional to the measurement uncertainty of mass, whereas the other quantities have a much lower effect being in the denominator of eq. S1. To quantify the measurement uncertainty of the mass measurement, the mass of an arbitrary chosen Kapton® sample was measured eleven times in a row, always resetting the scale (tare function) after every measurement. The results are shown in table S2. As Kapton® is slightly hygroscopic, room temperature, relative air humidity and ambient pressure are also provided. These quantities were measured with a Greisinger GFTB100 precision hygro- thermo- barometer with uncertainties of ± 2.5 % rel. H., ± 0.1 K and ± 1.5 mbar respectively.

Following the guidelines of the Guide for Measurement uncertainty (GUM) [26], the mass of the investigated sample had an arithmetic mean of 35.406 mg with a standard uncertainty of ± 0.007 mg. For a level of confidence of 95% this standard uncertainty has to be expanded by a factor of 2.23, to satisfy the fact, that the number of measurements was low and assuming a student's distribution. This means, that the overall uncertainty of this mass measurement was ±0.017 mg for a level of confidence of 95 %. In the following this value was assumed to be the uncertainty of all mass measurements with this scale.

Table S2: Investigation of the uncertainty of the mass measurement

n	m [mg]	θ [°C]	rel h. [%]	p [mbar]
1	35.405	17.4	46.4	1004.0
2	35.409	17.4	46.4	1004.0
3	35.401	17.4	46.4	1004.0

4	35.4	17.5	46.3	1004.0
5	35.401	17.5	46.2	1004.1
6	35.412	17.5	46.3	1004.1
7	35.399	17.5	46.1	1004.1
8	35.405	17.5	46.1	1004.1
9	35.417	17.5	46.0	1004.1
10	35.417	17.5	46.1	1004.1
11	35.403	17.6	46.1	1004.1

With these quantities clarified, three experiments were performed, in which two samples of Kapton®
200 HN were exposed for 24 h (n = 1, 2) and one sample (n = 3) was exposed for 48 h to atomic oxygen.

Table S3 shows the measurement results before (index 1) and after (index 2) the experiments. As the
samples immediately started to absorb humidity from the laboratory air, the final measurement was
performed after no change in mass could be observed over a time interval of 5 min. This condition was
achieved after 3 hours of waiting. In addition, the environmental parameters are provided to ensure
comparability.

Table S3: Measurement of mass of Kapton® samples before (index1) and after (index 2) atomic oxygen exposure

n	m_1 [mg]	θ_1 [°C]	rel h.$_1$ [%]	p_1 [mbar]	m_2 [mg]	θ_2 [°C]	rel h.$_2$ [%]	p_2 [mbar]
1	62.960	18.5	46.6	1001.0	62.870	19.2	43.9	990.5
2	36.169	18.7	46.3	1004.0	36.063	18.4	41.0	1006.3
3	71.376	18.7	43.8	1004.0	71.165	18.4	41.3	996.0

The environmental parameters were not exactly the same for the measurements. However, the values
are comparable, so that it is assumed that the environmental differences were well covered by the
measurement uncertainty, determined above.

The exemplary moisture absorption curve of sample 1 is shown in Fig. S2, indicating the hygroscope
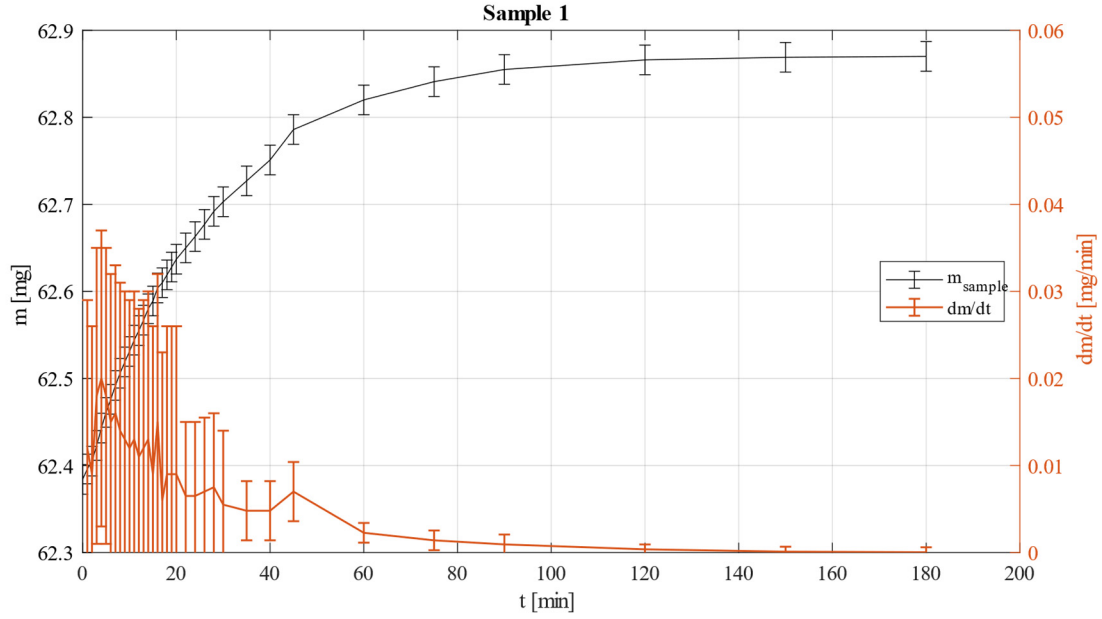nature of the samples.

Figure S2: Moisture absorption of Kapton® (sample 1) after the atomic oxygen exposure: Vertical bars indicate the measurement uncertainty; The measurement uncertainty of the time measurement of ± 1 s is not indicated

The measured mass differences, with the corresponding fluence and flux, calculated with eq. (S1) are presented in table S4.

Table S4: Mass difference, atomic oxygen fluence and atomic oxygen flux of the calibration experiments

n	Δm [mg]	F [Atoms/cm²]	t [s]	ϕ [Atoms/cm²s]
1	0.090 ± 0.034	$(2.10 \pm 0.79) \times 10^{19}$	86400 ± 60	$(2.43 \pm 0.92) \times 10^{14}$
2	0.106 ± 0.034	$(4.92 \pm 0.79) \times 10^{19}$	86400 ± 60	$(2.85 \pm 0.46) \times 10^{14}$
3	0.211 ±0.034	$(2.47 \pm 0.79) \times 10^{19}$	172800 ± 60	$(2.86 \pm 0.92) \times 10^{14}$

The results show that the ATOX test stand reproducibly provided a flux of atomic oxygen between $(2.43 \pm 0.92) \times 10^{14}$ Atoms/cm²s and $(2.86 \pm 0.92) \times 10^{14}$ Atoms/cm²s.

As the flux is determined, using the erosion rate of Kapton® in LEO, care has to be taken regarding the uncertainty of the above presented values. Although erosion of Kapton® in the laboratory with low velocities is comparable to LEO erosion according to NASA [27], the Kapton® erosion rate was provided without an uncertainty. Consequently, it is not considered in the propagation of measurement uncertainty above. The uncertainty of the mass difference is the doubled uncertainty of the mass measurement.

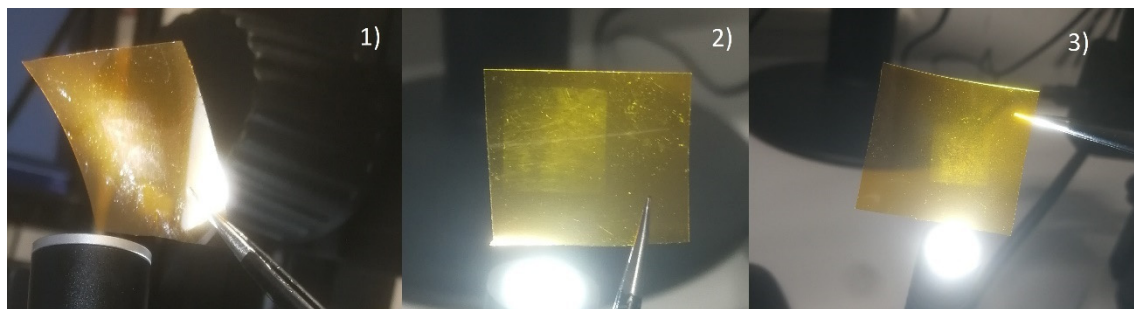Figure S3 shows the eroded area of the Kapton® samples, used for calibration.

Figure S3: Erosion area of Kapton® samples

The aluminium aperture, shown in Fig. S1, accurately restricted the area, being exposed to the atomic oxygen. An area of 1 cm² was degraded, so that in this area the samples' appearance seemed opaquer than in the rest of its surface.

Observing the eroded area with an incident light microscope as difficult because of the samples being transparent. This task would have been easier with a transmission light microscope. By applying a red, non-white substrate behind the sample, the erosion area was made more visible. This is shown in Fig. S4. The impression of colours in these images is distorted. However, the effect of erosion is visible in the form of more opaque patches, that have a milky look. In addition, a great number of scratch-like structures are observable. This raises the suspicion, that the material was eroded not only chemically but also mechanically. However, as can be seen in later in the test results of the test campaign, those scratches were not observed in any other surface, exposed to the atomic oxygen source. The scratches were therefore assumed to have been there already before the test, resulting from sample handling and storage.
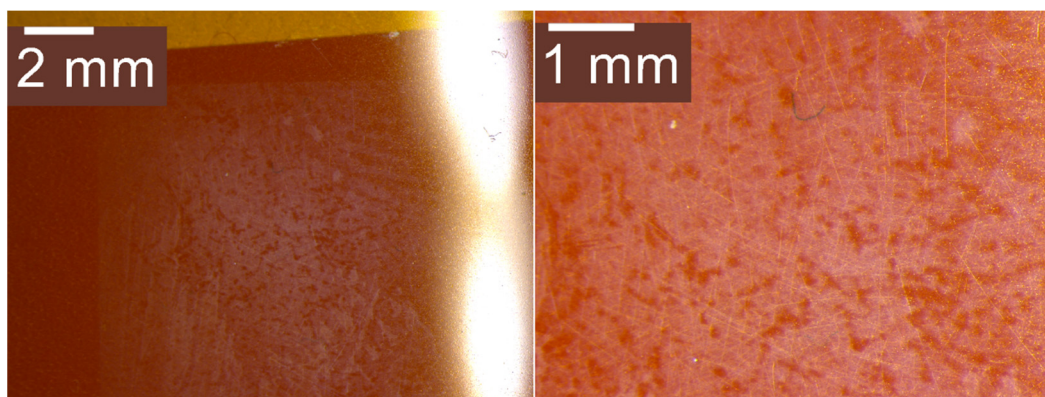

Figure S4: Images of the eroded surface of sample 3 under an incident light microscope; a red substrate was used to make the erosion more visible in comparison to a white substrate